Journal of Strain Analysis for Engineering Design, Vol. 45 (6), pp. 439-450, (2010).

Impact, penetration and perforation of a bonded CFRP composite panel by a high velocity steel sphere: an experimental study

PJ Hazell*, GJ Appleby-Thomas, G Kister

Cranfield Defence and Security, Cranfield University, Shrivenham, Swindon, Wiltshire, SN6 8LA, UK

ABSTRACT

In this work, the response of a bonded CFRP composite panel, manufactured by bonding two laminates together, to impact, penetration and perforation by a high-velocity steel sphere has been studied. The response of a relatively thick (c.a. 12 mm) laminate has been compared to similar data from [1] where relatively thin monolithic laminates were impacted by the same type of projectile. It was found that the ballistic performance of the system was increased over the impact energy range of interest when compared to these similar relatively thin composite laminates. Furthermore, both the energy absorbed per-unit-thickness of laminate and the level of damage as measure by C-Scan was similar when the panels were perforated at normal and oblique incidence. This raises the prospect of reducing experimental testing at oblique angles, if the behaviour at normal incidence is known.

Keywords: carbon fibre; ballistic impact; damage mechanics.

* Corresponding author: Email: p.j.hazell@cranfield.ac.uk; Tel: +44 (0)1793 785731

1.0 INTRODUCTION

Unlike metals and ceramics, there is a paucity of data on the high velocity impact and penetration behaviour of carbon fibre composite materials. Most of the work to date has concentrated on relatively low velocity impact studies [2-7] where the size and shape of the panel determine its energy absorbing capability. This is different to high velocity projectiles which induce a localised response in the target and consequently does not depend on the areal size of the target [8]. Most high velocity work with CFRPs to date has been done using single specimens of relatively thin laminates [9-14]. Some work has also been done on hybrid composites where fibre properties, sequencing and interfacial strengths have been varied [15,16]. However, little high velocity impact work has been done on relatively thick carbon fibre structures where the thickness of laminate was > 8 mm or on structures where two laminates were bonded together.

Bonded E-glass composite plates have however, been studied by Liu et al. [17]. In this work they studied the low velocity impact response of a variety of joining techniques with multiple layers of cross-ply laminates in an effort to understand the feasibility of replacing single thick laminates with multiple bonded thin laminates in structures. They concluded that pure epoxy bonding was found to be the most efficient joining technique in assembling composite laminates together since it gave the highest bending stiffness and perforation threshold. Furthermore, they showed that assembled composite plates were found to have perforation thresholds similar to the laminated counterpart. Consequently, they concluded that assembled composites could be used to replace the single laminates, as far as the perforation threshold was concerned.

Relatively few studies have also been done on the oblique penetration of CFRP laminates. Most impacts from high velocity projectiles will occur with some degree of obliquity and consequently, it is important to understand the effect that obliquity has on a penetrating projectile. Lamontagne et al. [18,19] have studied the penetration of CFRP laminates at oblique angles, however this was done at very high velocities that far exceeded the velocities of projectiles of interest in this study. More recently Lopez-

Puente et al. [14] have presented work on the normal and oblique penetration of CFRP laminates using both a gas gun and the finite element commercial code ABAQUS/Explicit. They showed that the maximum damage inflicted by the projectile at the ballistic limit was produced at normal incidence. Furthermore, below the ballistic limit, the extent of damage for normal impact was larger than that for the oblique impact. However, the extent of damage at higher velocities appeared to be greater for oblique impacts. Further oblique work has been presented in [1] where it was shown that for targets that were impacted at an oblique angle more of the kinetic energy was transferred from the projectile to the target material when compared to the same thickness of target that was subjected to a normal incidence impact. The authors also showed that this was merely due to a geometrical effect. Thicker panels appeared to behave more efficiently by absorbing more kinetic energy per effective-linear-thickness at the lower impact energies where petalling was a dominant factor in the penetration. This advantage seemed to vanish as the impact energy was increased.

In this study, the impact response of a two-part bonded woven CFRP where two 6-mm thick CFRP laminates were assembled using an epoxy adhesive was examined. The targets were subjected to impact and penetration by a fully-annealed stainless steel sphere within the velocity range of 187 m/s to 1219 m/s. This is the range of velocities that could be expected from small-arms bullets and fragments from exploding munitions. This corresponded to a kinetic energy range of between 126 J and 5324 J. Targets were placed at normal incidence to the axis of projectile flight and angled at 45°.

2.0 EXPERIMENTAL METHODOLOGY

2.1 Materials Used

The materials chosen for this study were woven CFRP laminates that were manufactured using the resin transfer method (RTM). These laminates were chosen because they are commonly used in the aerospace industry. All individual panels were manufactured with Hexcel G0926 Carbon Fabric with a 5 harness satin weave. The resin used was Hexcel

RTM 6 cured for 1 hour 40 minutes at 180 °C and at a pressure of 100 psi. The dynamic behaviour of the cured resin has previously been studied in [20-22]; the shock response of the laminate has been studied by Millett et al. [23] and Hazell et al. [24].The CFRP panel used in the two-part construction was 6 mm thick and made from 16 plies with the lay-up sequence from impact face: (0/90, ± 45, ± 45, 0/90, ± 45, ± 45, 0/90, 0/90, ±45, 0/90, ± 45, 0/90, ±45, 0/90, ± 45, 0/90). The targets were constructed by bonding two 300 mm × 300 mm panels of 6-mm thickness together using a two part epoxy adhesive (Hysol® 0151) under a uniformly distributed load of 2000 kgF at room temperature for 24 hours to provide a relatively thick structure (c.a. 12 mm) of symmetrical lay-up. The measured thickness of the adhesive layer ranged between 70 μm and 120 μm. The density of the CFRP material, measured using a Micrometrics AccuPyc 1330 gas pycnometer, was 1.512 g/cc ± 0.001 g/cc. The mass fraction of the reinforcement was measured using the acid digestion method according to ASTM D 3171-6, Procedure B [25] and was found to be 69.7±1.0%.

2.2 Impact testing

The projectile used was a fully annealed stainless steel sphere (∅11.97 mm ± 0.01 mm; mass = 7.165 g ± 0.001 g; VHN = 127). The balls (AISI 304) were fully annealed in air at 1050°C to provide equiaxed austenite grains and consequently isotropic behavior. The yield strength of this steel at 21°C is 450 MPa with an ultimate tensile strength of 675 MPa [26]. The projectile was fired from ELVIS, a single stage ∅22-mm gas-gun for velocities of less than 400 m/s. To achieve the higher velocities a 30-mm single stage gas gun and a ∅30-mm RARDEN cannon were employed. With the ∅30-mm gas gun, a baffle plate was employed behind the sabot stripper to remove any sabot debris that inadvertently made its way through the sabot stripper behind the projectile. Target specimens were cut from the bonded panels into 150 mm × 150 mm squares and secured at the top and bottom in a target–holding rig.

Impact, rebound, ricochet and exit velocities were measured by high-speed video camera (Phantom 7; 18,000 and 21,000 frames-per-second; 2 μs exposure time) to an accuracy of < 1%. The energy transferred to the panel (E_t) was calculated from

$$E_t = \frac{1}{2} m_p \left(v_i^2 - v_r^2 \right) \quad (1)$$

where m_p is the mass of the projectile, and v_i and v_r are the impact and residual velocities.

Consequently, the percentage change in kinetic energy (ΔE_f) was calculated using

$$\Delta E_f = \frac{E_t}{E_i} \times 100 \quad (2)$$

where E_i is the kinetic energy of the projectile prior to impact.

Parallax was taken into account by knowing the distances from the lens to the axis of penetration and from the axis of penetration to fiduciary markers.

The extent of damage in the perforated composites was assessed by doing C-scans using a glass reflector technique with a 5MHz, 50mm crystal focus transducer. Both the front plate and the rear plates were separately scanned. The scans were carried out by Midas NDT Systems Ltd. using a 1 mm grid and a scan speed of 100 mm/s.

3.0 RESULTS AND DISCUSSION

3.1 Change in energy

The change in the kinetic energy (KE) for the targets is shown below in Figure 1. For several low-energy cases, the projectile did not perforate the composite. Where the target was orientated at normal incidence to the trajectory of the projectile, impacting the

laminate target with an energy of 129 J (190 m/s) resulted in the projectile rebounding from the target with a relatively low velocity of 34 m/s. Increasing the impact energy resulted in the projectile rebounding at a lower velocity until the impact energy of 353 J (314 m/s) where the projectile was completely embedded in the back plate of the CFRP (see Figure 2). In this case, petalling was evident on the rear surface of the back plate. Eventually, perforation occurred with an impact energy of 429 J (346 m/s). This result implied a ballistic limit velocity in the range of 314 m/s – 346 m/s for the normal incident cases.

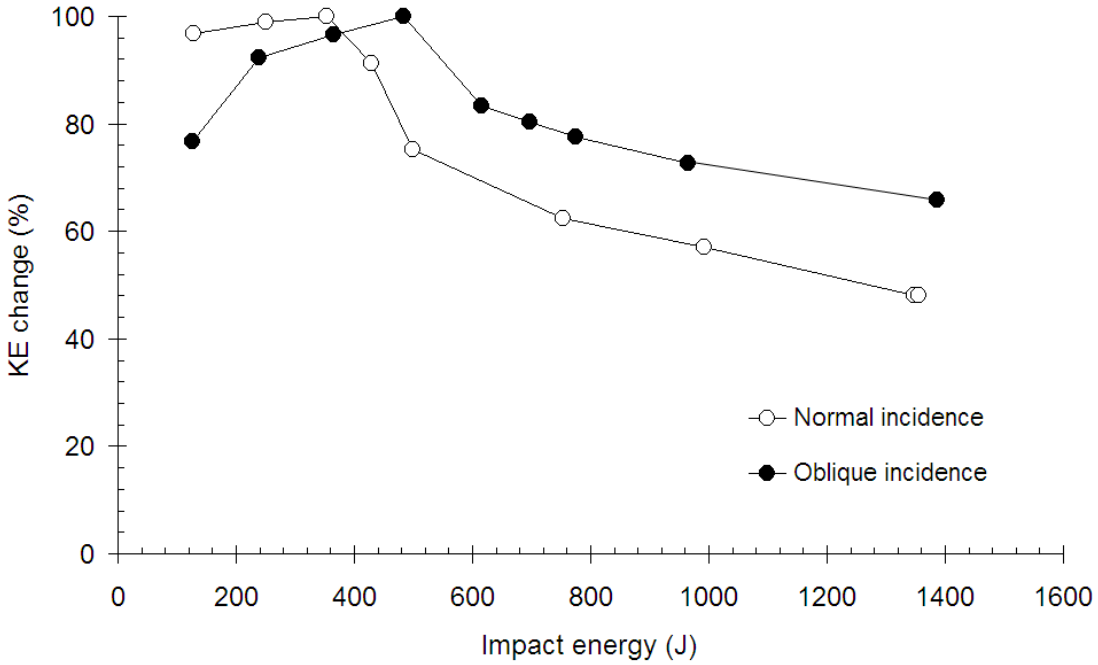

Figure 1: The effect of impact energy on the percentage change in kinetic energy of the projectile.

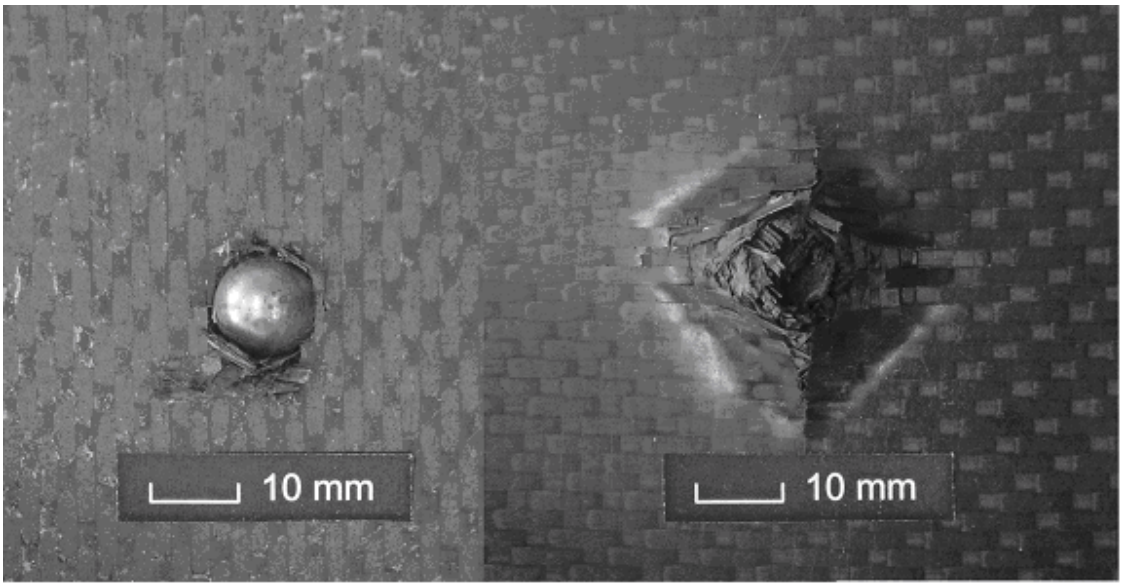

Figure 2: Front and rear surfaces (left and right respectively) of the second CFRP laminate plate after completely penetrating the front plate with an impact energy of 353 J (314 m/s).

After the perforation threshold was reached, increasing the impact energy led to a reduction in the percentage of kinetic energy transferred to the panel. This is in keeping with previous work [15,27] and corresponds to a reduction in the delamination of the structure (discussed later).

There is one further observation to note. Previous work [27] had shown that when a 6-mm thick composite of a similar lay-up to the panels tested here were subjected to impacts at velocities of up to 1875 m/s, an asymptotic level of kinetic energy absorption was achieved. For the normal incidence tests, we were able to achieve an impact velocity of 1219 m/s, corresponding to an impact energy of 5324 J (not shown in Figure 1). This test resulted in 36 % of the incident projectile energy being absorbed by the two-part bonded panel confirming that the percentage of kinetic energy absorbed was indeed approaching an asymptotic level.

For the oblique incident targets, increasing the impact energy from 126 J (188 m/s) resulted in an increase in the percentage of kinetic energy absorbed. In each case, the projectile ricocheted until the projectile became fully embedded in the target at 484 J (see Figure 3 (d)). Increasing the impact energy from 126 J to 239 J resulted in a relatively

rapid increase in the percentage of kinetic energy absorbed by the target when compared with further increases in impact energy. Figure 3(a) shows the effect on the target when the projectile strikes at 126 J. Very little material was removed from the target. Consequently, this resulted in a relatively high ricochet velocity. Increasing the impact energy from 126 J to 239 J (Figure 3(b)) resulted in more material being removed from the target with the penetration cavity increasing in length from 17.5 mm at 126 J impact to 23.3 mm at 239 J; the maximum depth penetrated increased from 1.7 mm at 126 J to 3.0 mm at 239 J. The ricochet velocity was reduced from 91 m/s to 71 m/s despite a higher impact velocity and this is consistent with the increase in amount of material excavated from the CFRP. Increasing the impact energy further to 365 J (319 m/s) resulted in a ricochet velocity of 60 m/s and a cavity length of 32.6 mm. The measured maximum depth-of-penetration in this case was 5.3 mm (see Figure 3c). Eventually, at an impact energy of 484 J (367 m/s), the projectile became fully embedded in the front plate (see Figure 3d). Only at this impact energy was the front plate completely penetrated. This was combined with visible failure of tows on the back face of the rear plate.

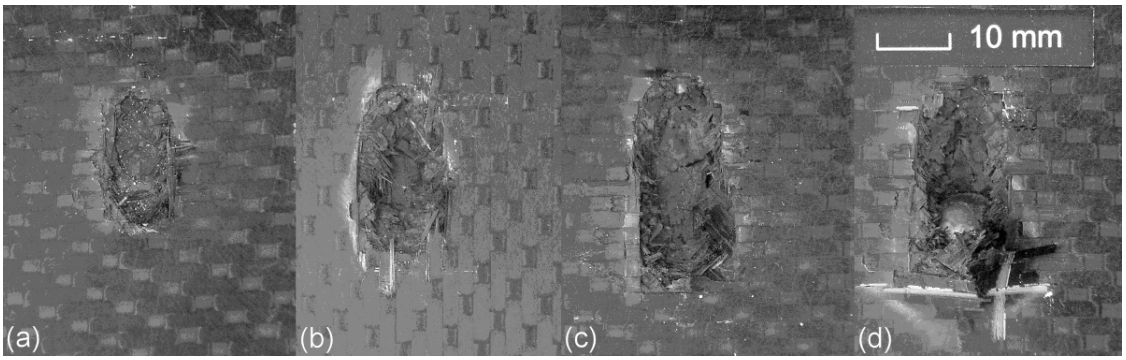

Figure 3: Penetration cavity formed after impacting the target with (a) 126 J (187 m/s), (b) 239 J (259 m/s), (c) 365 J (319 m/s), (d) 484 J (367 m/s).

There are two further things to note with the oblique targets. Firstly, the percentage of kinetic energy transferred to the oblique targets was consistently lower than that of the normal incident targets until perforation occurred at 429 J (346 m/s). This suggested that greater penetration and damage occurred in the normal incident targets when compared to the oblique targets until perforation. A comparison of the measured depth-of-penetration from recovered specimens that were subjected to similar impact velocities of 264 m/s and 258 m/s at normal and oblique angles respectively revealed that the normal incidence

impact specimen suffered c.a. 50 % more penetration than the oblique panel. At an impact energy of 484 J (367 m/s), the projectile penetrated the CFRP laminate target and became embedded resulting in 100% energy absorption (see Figure 3(d)).

Increasing the impact energy of the oblique targets to 615 J resulted in perforation. Interestingly, the behavior of the perforated oblique targets mirrored that of the normal-incident targets suggesting that similar penetration behavior was occurring. In each case however, a greater percentage of kinetic energy was absorbed by the oblique panels. This is a common feature of oblique targets that are subjected to ballistic impact. As noted in [1] for thinner targets (≤ 6 mm), this was due to the increase in effective linear thickness of material offered to the projectile. Figure 4 shows a direct comparison between the oblique experiments and normal incidence experiments. A linear trend line is fitted through the normal-incidence data. For the oblique targets the effective linear thickness offered to the projectile was calculated from

$$t_{eff} = \frac{t}{\cos\theta} \tag{3}$$

where t_{eff} is the effective linear thickness, t is the thickness of the laminate (nominally 12 mm) and θ is the angle between the trajectory of the projectile and the inclination of the target (nominally 45º).

As the impact energy is increased, there is negligible difference in the kinetic energy absorbed by the oblique target when the effective linear thickness is taken into account. Noticeably, the trajectory of the projectile did not deviate after it perforated the oblique targets again confirming that obliquity had negligible effect on the penetrating projectile. If the obliquity of the target was affecting the projectile's penetration path (by causing it to deviate during penetration) then the kinetic energy absorbed per effective-linear-thickness would be higher than that of the normal-incidence experiments and the projectile would deviate, usually exiting the target in a direction that was perpendicular to the plane of the target e.g., [28,29]. Consequently, over the impact velocity range of

interest, the oblique angle does not have any further effect on the resistance to penetration other than offering more material to penetrate.

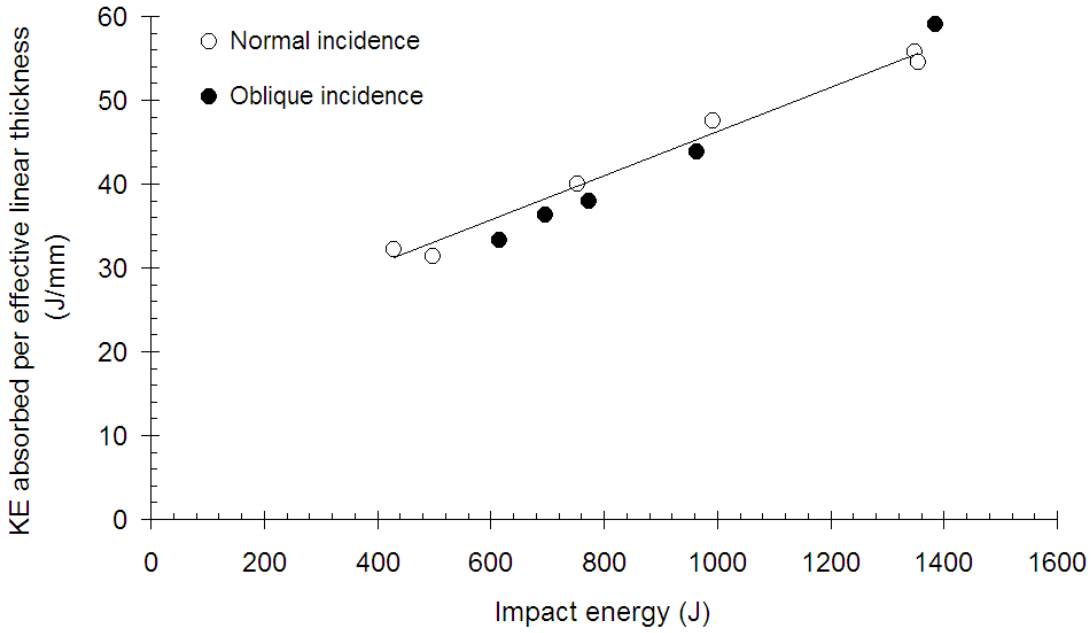

Figure 4: Comparison between normal and oblique incidence results where perforation had occurred.

3.2 Energy absorption per-unit-thickness

Figure 5 summarises the energy absorbed per-unit-thickness for targets that were perforated by the projectile. Only normal incidence cases are considered here due to a paucity of comparative oblique data. Additional data for the 6 mm and 3 mm composite materials is taken from [1] and [27]. The percentage of kinetic energy per-unit-thickness of material absorbed by the 12 mm thick CFRP is higher than the 6 mm and 3 mm examples when impacted at a similar range of energies.

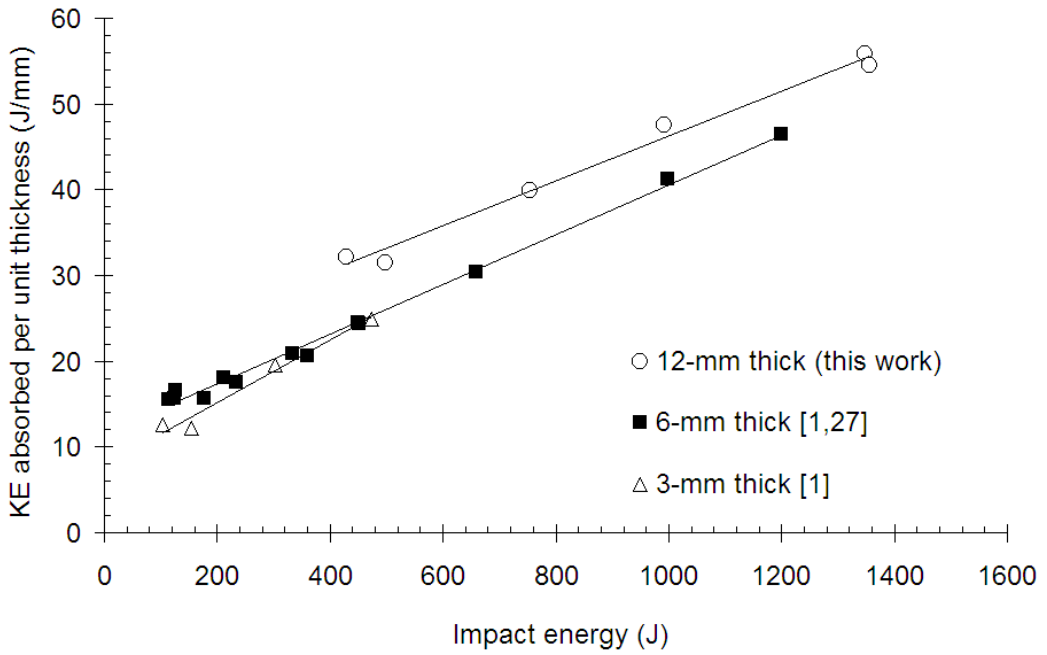

Figure 5: Absorbed energy-per-unit-thickness of CFRP where perforation of the target has occurred.

For the 3-mm and 6-mm thick composites, it is noted that the energy absorbed per-unit-thickness of material is similar whereas the 12-mm thick composites exhibit a slightly higher energy absorbing process. One possibility rationalisation for the observed result is that the distinct bonding layer inbetween the two laminates allows for the formation of a crushed zone of material from the front plate that spreads the load of the projectile over the backing plate. Petalling ensues (as opposed to plug-formation) leading to a larger amount of delamination in the rear plate. Indeed it was noticed that petalling of the rear plate was evident at impact energies of 992 J. Further tentative evidence for the relatively high ballistic performance of a two-part CFRP has also been shown with a non-woven laminate [30]. In this work, it was shown that the resistance offered by two 5.3-mm non-woven laminates that were bonded together provided a higher energy absorbing ability per-unit-thickness than a single 5.3 mm laminate.

Figure 6 shows the back-plates of several targets that have been perforated by the projectile. At the lower impact energies, it is clear that petalling occurs prior to

perforation. As the impact energy is increased, it is visible that (a) less petalling occurs and ; (b) the hole is clearly defined. Well defined holes are generally synonymous with shear-type failure [1] although it was evident that at the highest impact energy (5324 J) the clearly defined hole was due to particulation of the composite during projectile penetration [27].

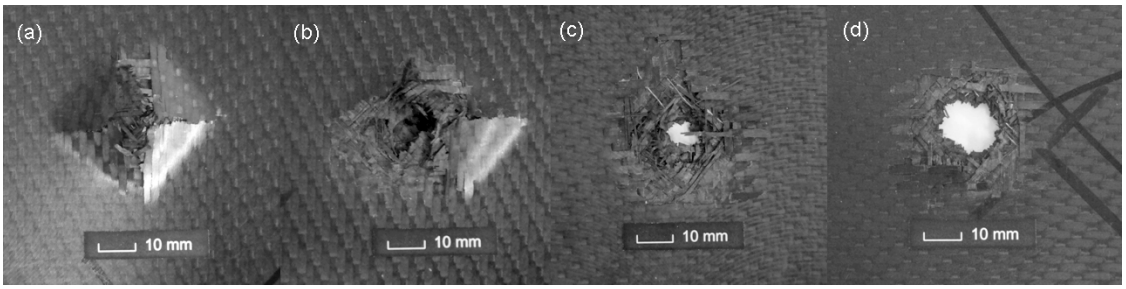

Figure 6: From petalling to particulation: the effect of the back-plate failure morphology as the impact energy is increased. The impact energies were as follows: (a) 429 J; (b) 498 J; (c) 992 J and; (d) 5324 J.

3.3 High-speed video results

3.3.1. No perforation

The sequence of events for the penetration of the normal target (353 J) and oblique target (365 J) are shown in Figures 7 and 8 respectively. In both cases, the projectile did not perforate the target. The time interval between each frame is 110 μs.

It is clear from Figure 7 that by 110 μs, the projectile had penetrated the two-part composite structure leading to ejecta from the front plate and petalling of the rear plate. By 330 μs, it was evident that the glue layer, bonding the two samples together, had failed resulting in separation of the plates. Ultimately, by 550 μs, a small plug of CFRP was ejected from the rear of the plate.

Figure 8 shows the penetration of the steel sphere into an oblique target. By 110 μs, bulging of the rear plate is evident in a direction that is perpendicular to the plane of the target. This has been previously observed with monolithic laminates of thickness 3 mm and 6 mm [1]. This suggests that delamination in the rear panel occurs mostly

symmetrical. However by 220 μs, the rear panel is seen to recover. By 330 μs, it appears that a large amount of debris has been ejected from the front plate; by 440 μs the projectile is seen to ricochet in the general direction of the plane of the target. Although it is not obvious in these images, delamination of the rear plate from the front plate occurred as observed with the normal incidence target.

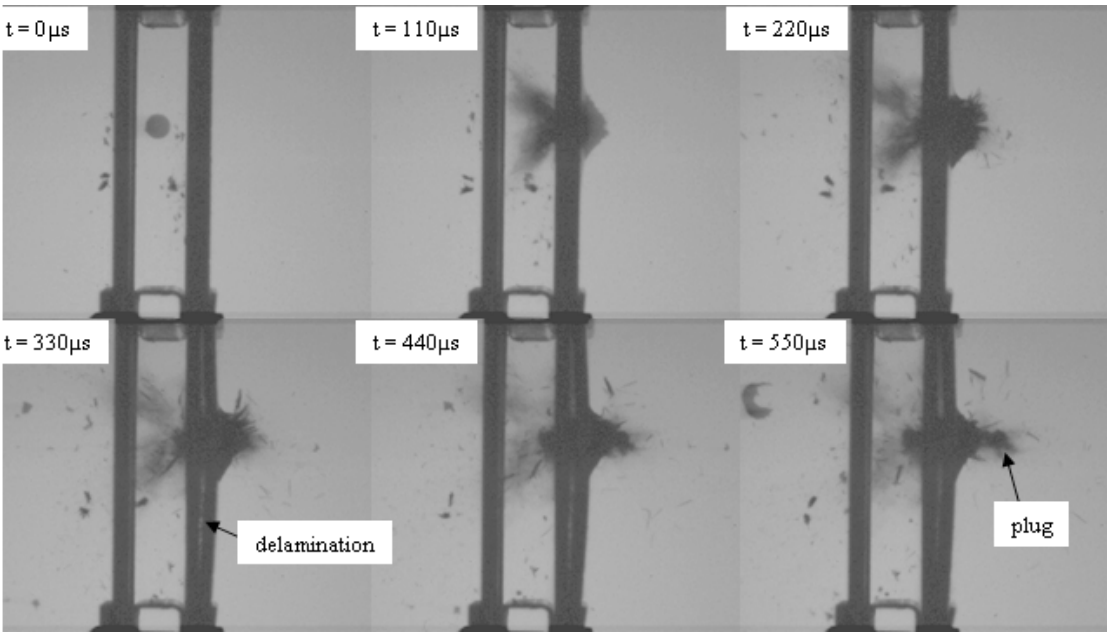

Figure 7: Impact of a normal incidence target at 353 J (314 m/s).

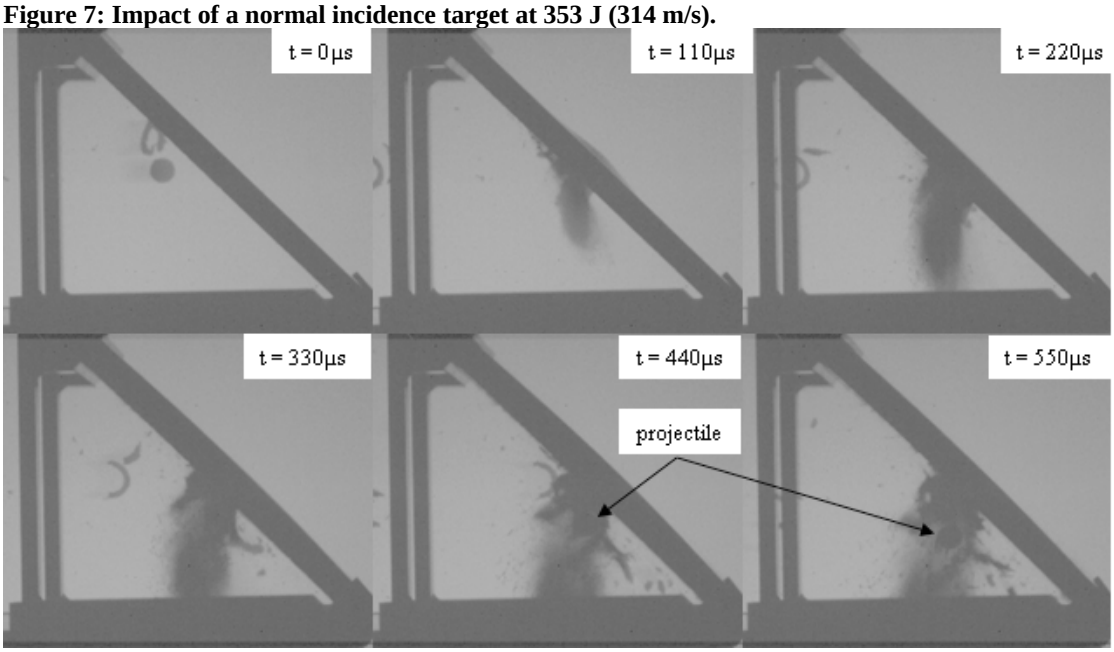

Figure 8: Impact of an oblique incidence target at 365 J (319 m/s).

During penetration the adhesive line of all the targets except the oblique target that was struck at 126 J (188 m/s) failed leading to separation of both plates. For the sample shown in Figure 7 (E_i = 353 J), interrogation of the high-speed video showed that by 220 μs after impact, the rear plate became separated from the front plate. A small degree of bending ensued.

There are two possibilities as to why the bonding layer failed during penetration. Firstly, stress wave reflections at the interface could give rise to tensile instability within the adhesive layer. However, this only becomes evident when there is an impedance mismatch between samples [31]. The shock impedance for the RTM6 resin used in the manufacture of these composite materials is very similar to common epoxy resins [20] and therefore it is very unlikely that this was the cause. It is more likely that the failure is dominated by shear-failure processes and the localised movement of the rear plate away from the front plate due to the petalling process that ensues. Due to the low strain-to-failure of the resin used to bond the samples together (c.a. 2.4% [32]), any localised movement in the rear plate caused by the penetrating projectile would result in failure of the bond layer.

3.3.2 Perforation

The sequence of events for the penetration of the normal target (429 J) and oblique target (615 J) are shown below in Figures 10 and 11 respectively. Each of these Figures represents the results for the lowest energy impact to induce perforation of the laminates. In these cases, the time interval between each frame is 55 μs and 48 μs for the normal-incidence and the oblique-incidence tests respectively.

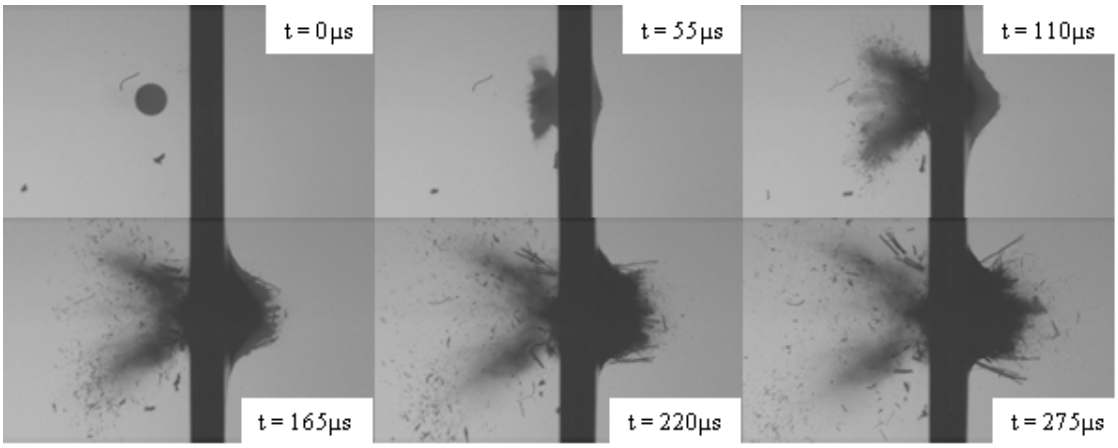

Figure 9: Perforation of a 12-mm thick two-part laminate; impact energy = 429 J (346 m/s).

Figure 10 shows the effect of the sphere penetrating and then perforating the two-part laminate. By 110 μs, symmetrical deformation of the rear laminate is visible as the projectile penetrates the front laminate finally resulting in tensile failure and break-out by 165 μs. Unlike, the 6-mm thick composites impacted with a similar kinetic energy [1], no plug was formed; instead the rear of the target failed via petalling with the rear of the panel showing a similar failure mode to the sample impacted at 353 J (see Figure 2). The petals that were formed were pushed apart by the penetrating projectile and eventually relaxed, partially closing up the penetration cavity. It was evident that relatively few fragments were formed as the projectile exited the target.

The effect of obliquity on the penetration mechanisms is shown in Figure 10. As with the target that was not perforated, the rear laminate deformed in a direction that was perpendicular to the plane of the laminate. When perforated, some debris was propelled in that direction whereas the projectile continued along its pre-impact trajectory.

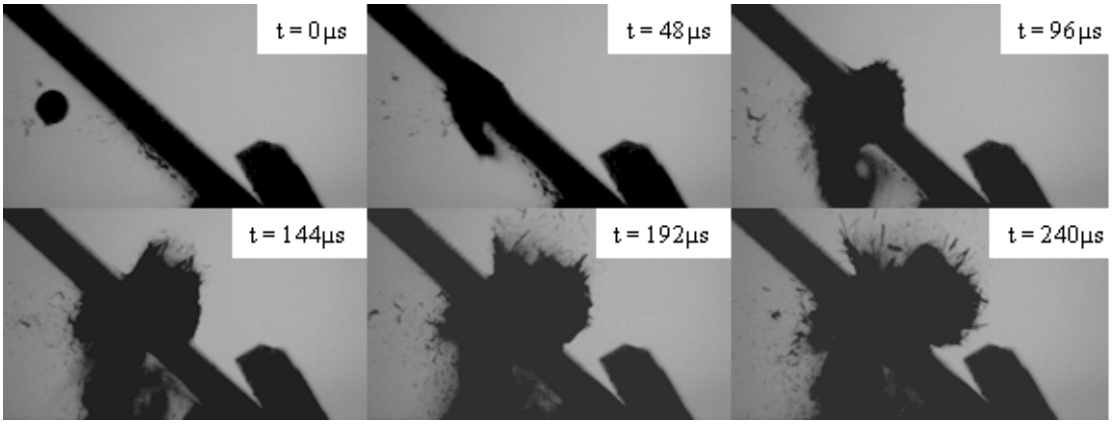

Figure 10: Perforation of a 12-mm thick two-part oblique laminate ; impact energy = 615 J (414 m/s). Here, the frame rate for the camera has been increased to 21,000 fps.

3.4. Damage assessment

The targets were C-scanned to examine the extent of the damage to the panels. An image analyzer program was used to measure the damage zone when the signal attenuation was greater than 5 dB. For the targets impacted at a velocity close to the minimum required to perforate the target, the cavity had partially closed therefore giving a misleading representation of the size of the penetration channel. Consequently, the results presented in Figures 12 and 13 include the hole size and represent the total area of damage. It was noted that in the majority of the normal incidence impact cases the area of delamination was mostly circular for both the front and rear panels. For the oblique samples at the lower impact energies, the mostly circular shape implied that symmetric localised deformation had occurred. These observations were different to what was seen with the 3 mm and 6 mm thick targets [1] where the impact energy was sufficient to cause asymmetric damage at oblique angles. However where the projectile became fully lodged in the sample (E_i = 484 J) the C-scan revealed that the delamination was wider at the top of the penetration channel (see Figure 3(d)) resulting in a non-circular pattern whereas the rear panel showed a mostly circular pattern. A similar pattern was shown as the projectile perforated the target.

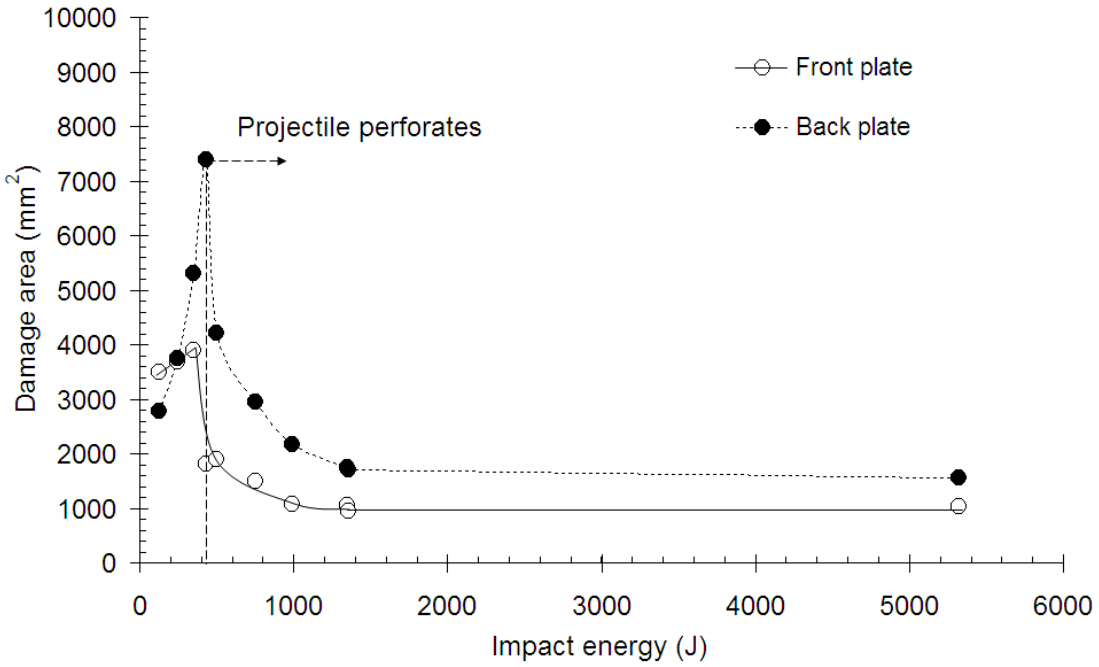

Figure 11: Damage area as measured by C-scan for the targets struck at normal incidence.

Although we must be cautious in drawing too many conclusions from these results because these scans provide a two-dimensional view of damage instead of a full three-dimensional picture, there are a number of observations to note here. Figure 11 shows the separate C-scans for both the front and back plates for the targets that were subjected to normal incidence impact. For the back plate, the amount of damage increased with impact energy and was greatest (for the impact energy range of interest) at 429 J (346 m/s). At this energy, the projectile just perforated the target. This increase in damage area in the back plate was consistent with an increased level of deformation and petal formation as the projectile penetrated deeper into the front plate. However, the damage in the front plate changed little over the impact energy range of 129 J – 353 J. When the target was perforated with an impact energy of 429 J, the level of damage in the front plate dropped whereas in the backplate, a high level of damage was recorded consistent with a high level of localised bending and petalling. A drop-off in damage area with increasing impact energy has also been seen in [1] when monolithic composite laminates were subjected to impact and penetration. In this work a drop-off in damage area was characteristic of a change of penetration mechanism from that of petalling to that of

plugging. It should also be noted that when the panel is perforated, although the damage does decrease with increasing impact energies, the degree of impact energy absorbed increases (see Figures 4-5). This has previously been shown to occur with 6-mm thick laminates [1, 27] and has been shown to be due to energy being used to form larger cavities, greater particulation in the penetration zone and the transfer of energy to the KE of the resulting fragments [27].

Despite the fact that compressive /shear failure had occurred in the front plate of the CFRP laminate, the level of damage as measured by C-scan, was considerably higher for the front plate of these two-part laminates than a single 6-mm thick laminate that was impacted at similar velocities. From data in [1], the level of damage for the 6-mm thick composite in the impact energy range of 200 J to 400 J was c.a. 1500 mm^2. Whereas, for the 12-mm bonded samples, the level of observed damage in the front panel was 3700 mm^2 in a similar impact energy range. Consequently, bonding the second layer of CFRP laminate behind a target laminate not only increases the ballistic performance of the system but also leads to an increase in the damage to the front plate. Damage to the back plate was considerably more extensive too when compared to the single 6-mm thick laminates. Here we saw an increase in the level of damage where petalling was the dominant factor.

For the oblique targets, the damage area is shown in Figure 12. Here the behaviour of the front plate was different to that seen with the normal incidence impacts. The initial dashed line used to link the initial two data points for the front plate (from 126 J → 239 J) is assumed and therefore should be treated with a degree of caution. Nevertheless, it is clear that there is a relatively steep rise in the front plate damage as the impact energy is increased from 126 J to 239 J. At 126 J (188 m/s), the delamination in the front plate was small (c.a. 1380mm^2). Increasing the impact energy resulted in an increase in delamination until the projectile penetrated deep into the front plate (at 365 J / 484 J). This resulted in less delamination. It should be pointed out however, that at an impact energy of 126 J (188 m/s), there was insufficient energy to separate the plates during impact. Consequently, this resulted in a much stiffer structure, restricting the amount of

delamination and leading to a much higher ricochet velocity and therefore less energy absorption by the plate (see Figure 1).

Prior to perforation there are a few things to note. With the rear plate the recorded damage increased with the impact energy and was consistently less than the damage incurred at normal incidence. This is consistent with the result shown in Figure 1 where the percentage of kinetic energy absorbed by the plate at the oblique angle is less than at normal incidence. That is until perforation occurs. This is also consistent with the work of Lopez-Puente et al. [14] who showed that with thin (c.a. 2.2 mm) woven laminates, below the ballistic limit the extent of damage was higher in targets struck at normal incidence when compared to those that were struck at oblique incidence. This was due to the projectile being ricocheted from the composite plate instead of rebounding. That is, not all of the kinetic energy is being imparted into the plate but rather the energy is being deflected by the oblique plate resulting in less damage.

After perforation, however the level of the damage in both the front plate and the rear plate is similar for both the normal-incidence cases and oblique-incidence cases (see Figure 13). Therefore both the level of damage and the KE absorbed per-unit-thickness is similar for the normal and incident targets. This raises the prospect that with these types of materials it is possible to understand the behaviour of an obliquely struck laminate from a single test at normal incidence.

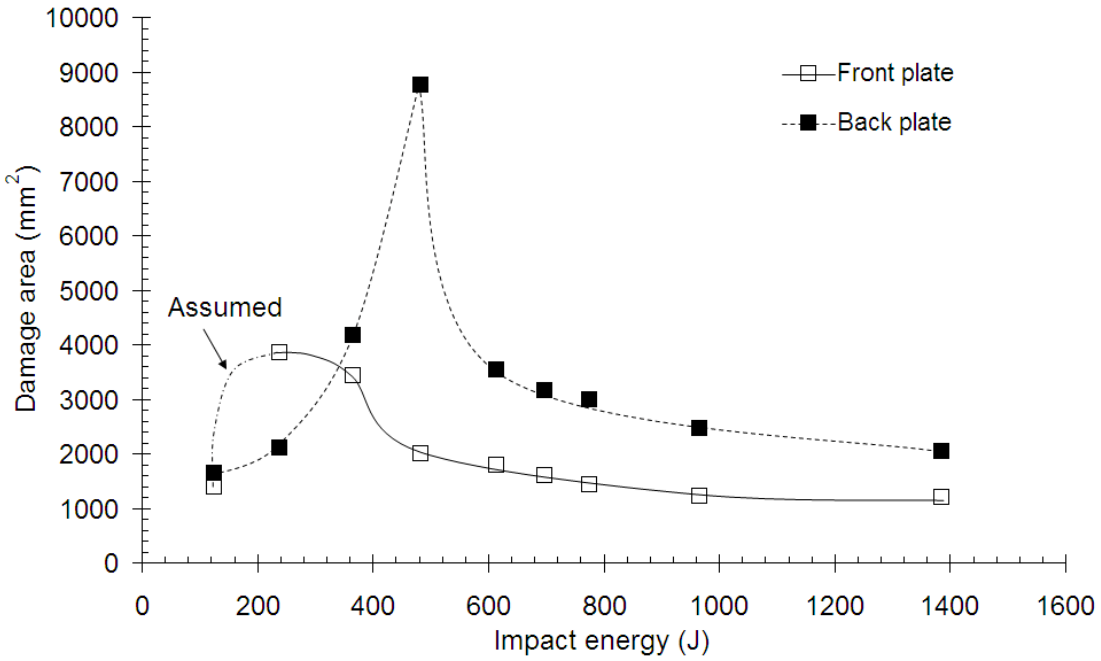

Figure 12: Damage area as measured by C-scan for the targets struck at oblique incidence.

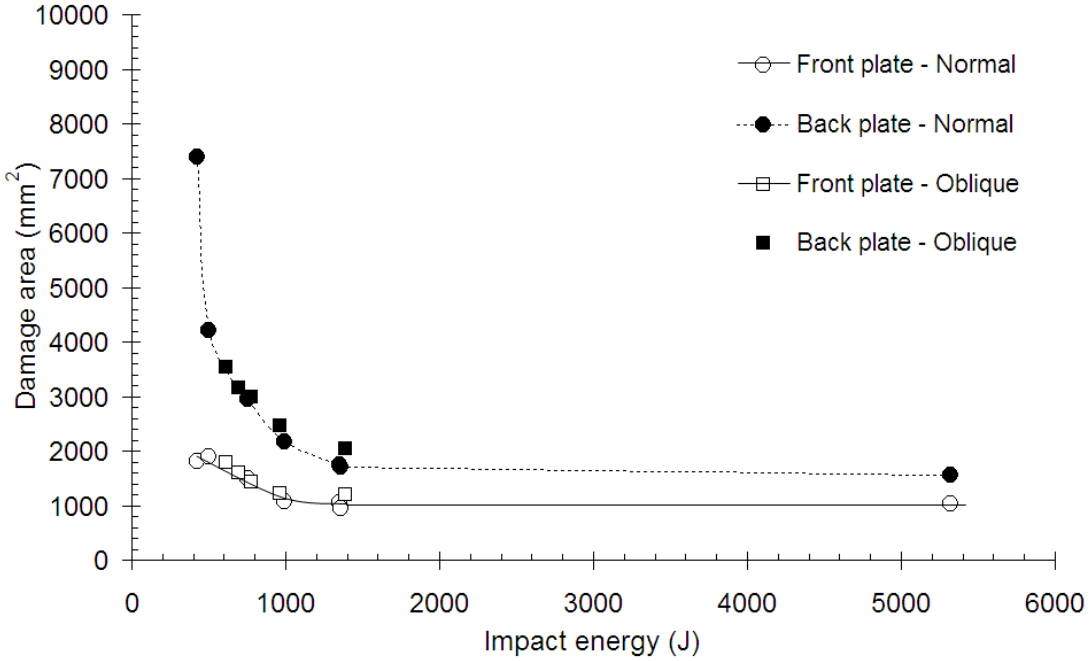

Figure 13: Comparison between the level of damage (as measured by C-scan) for both the front plate and rear plate; after perforation.

4.0 CONCLUSIONS

Two 6-mm thick CFRP laminates have been bonded together to evaluate the ballistic performance of such a system when subjected to impact and penetration by a ∅12-mm stainless steel projectile at velocities ranging from 187 m/s to 1219 m/s. The following conclusions are drawn from the data:

(1) Over the impact velocity range of interest, an obliquely-angled target does not have any further effect on the resistance to penetration other than offering more material to penetrate. Furthermore, once the panel was perforated, the level of damage, as measured by C-Scan for both the front plate and rear plate, was similar. This raises the prospect of reducing experimental testing at oblique angles, if the behaviour at normal incidence is known.

(2) It was found that the ballistic performance of the two-part system was improved compared with similar thin CFRP laminates over the impact energy range of interest. Further, this improvement on the ballistic performance occurred with an increase in damage when compared to thinner laminates.

(3) During oblique penetration, the rear plate deformed in the direction perpendicular to the plane of the laminate. This resulted in a mostly circular delamination pattern whereas the front plate suffered asymmetric damage.

(4) Failure of the adhesive bonding layer occurred for all targets except on an oblique target struck at the lowest impact energy. This was most likely due to shear-induced failure processes occurring at the bond line and localised separation of the rear CFRP laminate plate as petalling ensued.

5.0 ACKNOWLEDGEMENTS

Part of this work was carried out during Mr Pierre Bourque's Military Vehicle Technology MSc course and consequently we are very grateful for his contribution. We would also like to acknowledge Mr Gary Cooper who helped with some of the experimental tests. The authors would like to thank Mr Keith Campbell of Short Brothers

plc, Belfast, UK for supplying the CFRP panels. We also gratefully acknowledge the UK MoD and the EPSRC who funded part of this work under GR/S33994/01.

6.0 REFERENCES

1. Hazell PJ, Kister G, Stennett C, Bourque P, Cooper G. Normal and oblique penetration of woven CFRP laminates by a high velocity steel sphere. Compos Part A-Appl S 2008; 39:866-874.
2. Cantwell WJ, Morton J. The impact resistance of composite materials — a review. Composites 1991;22(5):347-362.
3. Richardson MOW, Wisheart MJ. Review of low-velocity impact properties of composite materials. Compos Part A-Appl S 1996;27(12):1123-1131.
4. Morton J, Godwin EW. Impact response of tough carbon fibre composites. Compos Struct 1989;13:1-19.
5. Cantwell WJ, Curtis PT, Morton J. An assessment of the impact performance of CFRP reinforced with high-strain carbon fibres. Compos Sci Technol 1986; 25(2):133-148.
6. Curtis PT, Bishop SM. An assessment of the potential of woven carbon fibre-reinforced plastics for high performance applications. Composites 1984;15(4):259-265.
7. Robinson P, Davies GAO. Impactor mass and specimen geometry effects in low velocity impact of laminated composites. Int J Impact Eng 1992;12(2):189-207.
8. Cantwell WJ, Morton J. Comparison of the low and high velocity impact response of CFRP. Composites 1989;20(6): 545–551.
9. Bland PW, Dear JP. Observations on the impact behaviour of carbon–fibre reinforced polymers for the qualitative validation of models. Compos Part A-Appl S 2001;32:1217–1227.
10. Hammond RI, Proud WG, Goldrein HT, Field JE. High-resolution optical study of the impact of carbon-fibre reinforced polymers with different lay-ups. Int J impact Eng 2004;30:69-86.
11. Tanabe Y, Aoki M. Stress and strain measurements in carbon-related materials impacted by high-velocity steel spheres. Int J Impact Eng 2003;28:1045-1059.
12. Cantwell WJ, Morton J. Impact perforation of carbon fibre reinforced plastics. Compos Sci Technol 1990;38:119-141.
13. Hosur MV, Vaidya UK, Ulven C, Jeelani S. Performance of stitched/unstitched woven carbon/epoxy composites under high velocity impact loading Compos Struct 2004;64:455–466.
14. Lopez-Puente J, Zaera R, Navarro C. Experimental and numerical analysis of normal and oblique ballistic impacts on thin carbon/epoxy woven laminates. Compos Part A-Appl S 2008;39:374-387.
15. Tanabe Y, Aoki M, Fujii K, Kasano H, Yasuda E. Fracture behavior of CFRPs impacted by relatively high-velocity steel sphere. Int J Impact Eng 2003;28:627-642.
16. Fujii K, Aoki M, Kiuchi N, Yasuda E, Tanabe Y. Impact perforation behavior of CFRP using high velocity steel sphere. Int J Impact Eng 2002;27:497–508.
17. Liu D, Raju BB, Dang X. Impact perforation resistance of laminated and assembled composite plates. Int J Impact Eng 2000; 24:733-746.
18. Lamontagne CG, Manuelpillai GN, Taylor EA, Tennyson RC. Normal and oblique hypervelocity impacts on carbon fiber composites. Int J Impact Eng 1999;23:519–532.
19. Lamontagne CG, Manuelpillai GN, Kerr JH, Taylor EA, Tennyson RC, Burchell MJ. Projectiles density, impact angle and energy effects on hypervelocity impact damage to carbon fiber/peek composites. Int J Impact Eng 2001;26:381–398.
20. Hazell PJ, Stennett C, Cooper G. The shock and release behaviour of an aerospace-grade cured aromatic amine epoxy resin. Polym Composite 2008; 29 (10):1106-1110.
21. Gerlach R, Siviour CR, Petrinic N, Wiegand J. Experimental characterisation and constitutive modelling of RTM-6 resin under impact loading, Polymer, 49 (11): 2728-2737.
22. Appleby-Thomas GJ, Hazell PJ, Stennett C. The variation in lateral and longitudinal stress gauge response within an RTM 6 epoxy resin under one-dimensional shock loading, J Mater Sci., doi:10.1007/s10853-009-3859-z.
23. Millett JCF, Bourne NK, Meziere YJE, Vignjevic R, Lukyanov A. The effect of orientation on the shock response of a carbon fibre-epoxy composite, Compos Sci Technol 2007;67:3253–3260.

24. Hazell PJ, Stennett C, Cooper G. The effect of specimen thickness on the shock propagation along the in-fibre direction of an aerospace-grade CFRP laminate. Compos Part A-Appl S 2009; 40 (2):204-209.
25. ASTM Standard D 3171-06. Standard Test Methods for Constituent Content of Composite Materials. ASTM International, 2006.
26. Cryogenic materials data handbook, Volume 1, Sections A-C, Air Force Materials Laboratory, Air Force Command, Wright-Patterson Air Force Base, Ohio, AFML-TDR-64-280, 1970.
27. Hazell PJ, Cowie A, Kister G, Stennett C, Cooper GA. Penetration of a woven CFRP laminate by a high velocity steel sphere impacting at velocities of up to 1875 m/s. Int J of Impact Engng 2009; 136 (9):1136-1142.
28. Goldsmith W, Finnegan SA. Normal and oblique impact of cylindro-conical and cylindrical projectiles on metallic plates. Int J Impact Engng 1986; 4 (2): 83-105.
29. Gupta NK, Madhu V. An experimental study of normal and oblique impact of hard-core projectile on single and layered plates. Int J Impact Engng 1997;19:395-414.
30. Hazell PJ, Appleby-Thomas GJ. A study on the energy dissipation of several different CFRP-based targets completely penetrated by a high velocity projectile. Compos Struct 2009; 91:103-109.
31. Meyers MA. Dynamic Behavior of Materials, John Wiley, New York, 1994.
32. Loctite Hysol® 0151 Product Description Sheet, 1001 Trout Brook Crossing, Rocky Hill, CT 06067-3910 (May 2002).